South African Journal of Geomatics, Vol. 10. No. 1, February 2021

Assessment of Positional Accuracies of UAV-Based Coordinates Derived from Orthophotos at Varying Times of the Day- A Case Study

S. Mantey, M. S. Aduah

Department of Geomatic Engineering, University of Mines and Technology, P. O. Box 237, Tarkwa, Ghana, smantey@umat.edu.gh, msaduah@umat.edu.gh

DOI: http://dx.doi.org/10.4314/sajg.v10i1.4

Abstract

Positional accuracy is one of the important factors which determines acceptability of survey work. Apart from the equipment and method used which affect the accuracy of surveys, time of the day in which the equipment operates can equally affect the accuracy of a survey. In this study, the performance of Unmanned Aerial Vehicle (UAV) surveys as well as the appropriate time in the day to apply the technology in Tarkwa, Ghana, has been investigated. The paper assessed the positional accuracies of ground features on UAV-based orthophotos (with emphasis on horizontal coordinates), captured at different times of the day, keeping all other parameters unchanged for capturing, production and processing of all orthophotos each time. The positional accuracies of selected features on the orthophotos were determined by calculating the Root Mean Square Error (RMSE) between the feature coordinates on the ground measured with GNSS Receivers and those derived from the UAV-based orthophotos. The results show that coordinates derived from orthophotos captured in the morning, with average temperatures between 21 ℃ and 23 ℃, and average wind speed of not more than 10 m/s, produced images with the highest positional accuracies, with RMSE values between 0.0047 m and 0.0283 m. These RMSE are within the range of values recommended for standard mapping surveys as well as GIS.

Keywords: *UAVs, RMSE, Accuracy, DSM, orthophotos, Ground Control Points, Coordinates*

1. Introduction

Accuracy is one of the most important factors of land surveys. The purpose of land survey is to accurately determine or establish relative positions of points above, on or beneath the Earth surface (Chauhan *et al*., 2006). Although accuracy of land surveys is very important, surveys have not always been as accurate as they are now as a result of technological advancement in the land survey profession (Anon., 2019a). Over the years, the fundamental basics of land surveying have hardly changed, however, the technology and methods used have advanced along with the accuracy of surveying. This makes the equipment and methods used an important element that affects the accuracy of surveying. Another important factor that affects the accuracy of land surveying given a

particular equipment is the weather condition in which the equipment operates (Anon., 2014). Both traditional and modern equipment used in land surveying performs well in terms of accuracy under certain weather or atmospheric conditions which occur differently at various times of the day. Windy condition decreases the stability of theodolites, total stations, prisms and plumb bobs thereby decreasing their performance in terms of accuracy (Anon., 2019b). Hot temperatures in sunny hours strike certain parts of equipment which may cause differential expansion in the metal components resulting in small errors. For example, night observations are recommended when using GPS receivers since dominant error sources such as ionospheric and tropospheric delays do not affect positions as strongly as they do during the day time (Abubakar *et al*., 2017).

Unmanned Aerial Vehicle (UAV), according to the Unmanned Vehicle Systems (UVS) international definition, is a generic aircraft designed to operate with no human pilot onboard. Recent development in sensors and flying platforms has significantly broadened their application (Raczynski, 2017) and their usage in land surveying has become a common practice. Often, the limiting factor for UAV is the weather conditions (Hakala *et al.,* 2013). Sunlight affects the quality of the images that are taken, and too bright or dark lightning can lead to difficulties for software in post-processing and aligning the photos (Leitão *et al.,* 2016). It has been shown that weather decreases the radiometric quality of images. Low quality photographs directly affect the bundle adjustment results together with accuracy and density of generated point clouds and the generated Digital Terrain Model, consequently reducing the accuracy of orthophotos and extracted coordinates (Wierzbicki *et al.,* 2015). Although, no measurement in a survey is exact (Chauhan *et al*., 2006), errors must be kept to a minimum as possible. This study seeks to investigate the appropriate time of the day to achieve the highest positional accuracy when using UAV surveys with emphasis on horizontal coordinates.

1.1. Unmanned Aerial Vehicles (UAVs)

UAVs are uninhabited and reusable motorised aerial vehicle (Blyenburgh, 1999). These vehicles are either remotely controlled, semi-autonomous, autonomous, or have a combination of these capabilities. Comparing to the manned aircraft, the main difference between the two systems is that UAV requires no pilot to be physically present in the aircraft according to the Unmanned Vehicle Systems (UVS) International definition. This, however, does not imply that UAV flies by itself autonomously. In many cases, the crew (operator, back-up pilot *etc*.) responsible for a UAV is larger than that of a conventional aircraft (Everaerts, 2008). The term UAV is used commonly in the Geomatics and Computer Science, Robotics and Artificial Intelligence, as well as the Photogrammetry and Remote Sensing communities. However, synonyms such as Remotely Piloted Vehicle (RPV), Remotely Operated Aircraft (ROA), Remote Controlled (RC) Helicopter, Unmanned Vehicle Systems (UVS) and Model Helicopters are often used (Eisenbeiss, 2009). Recent UAVs are equipped with several units and sensors, which has become an integral part of the UAV and helps in the photogrammetric process. To be able to perform autonomous flight with predetermined waypoints or path, a GNSS receiver is introduced in the design of UAV. GNSS is not only used for the autonomous steering but also for georeferencing the images. Currently, Real Time Kinematics (RTK)

GNSS are being tested for their ability to perform direct georeferencing in order to eliminate or reduce the necessity of using Ground Control Points (GCPs). Similarly, Inertial Navigation System (INS) and Inertial Measurement Unit (IMU) play important roles in the quality of a flight. INS consist of motion sensors (accelerometers), rotation sensors (gyroscopes) and magnetometers. IMU is responsible for collecting data about forces acting on the aircraft. There is also the presence of a barometer, which determines the actual altitude of UAV over the starting point and they altogether are essential for fixing UAV's position and providing highest possible accuracy of a final product (Koeva *et al.,* 2018). Similar to other aircraft, unmanned vehicles must always fly in a safe manner, both with respect to people and properties on the ground and also to other UAVs. Regulations are therefore enforced to ensure public safety (Eisenbeiss, 2009). Unmanned Aerial Vehicles are widely used in many applications for different purposes. Recent developments in sensor and flying platforms have significantly broadened their application (Raczynski, 2017). While their application in military operations was perhaps their first use, the industry of civil UAVs has been increasing steadily, and has more than doubled since 2008 (Leitão *et al.,* 2016). UAVs are now used in land surveying (Mantey and Tagoe, 2019; Manyoky *et al*., 2011; Volkmann and Barnes, 2014), precise agriculture for crop monitoring, spraying and health assessment of vegetation, in archaeology for documentation of excavations (Thomas, 2016) or in photogrammetry for 3D modeling (Colomina and Molina, 2014). They have also found application in Search and Rescue services and also in the entertainment or movie industry.

1.2. Effect of Weather on Performance of UAVs

Often, the limiting factor for UAVs is the weather conditions (Hakala *et al*., 2013). According to Raczynski (2017), weather conditions affect the performance a photogrammetric flight and does not necessarily depend on the UAV operator. Strong wind disturbs UAV in realising a perfect, pre-planned flight projects. Small aircraft are also vulnerable to wind gust which can result in "holes" in overlap between images. Sunlight affects the quality of the images that are taken and too bright or dark lightning can lead to difficulties for software in post-processing the photos. Lighting and the presence of shadows may have a strong effect on photogrammetric results (Leitão *et al.,* 2016). At the data acquisition stage for orthophoto production, weather condition among other factors such as the camera exposition parameters (shutter speed, aperture value) have a considerable impact on the final image quality. Other factors determining geometric accuracy are the motion blur and the image inclination angle effects. These are also caused by the vehicle flight stability, which can possibly be disturbed by weather parameters (turbulence, sudden wind flows *etc*.). Poor weather decreases the radiometric quality of images taken by UAVs. Low quality images directly affect the bundle adjustment results and accuracy of generated point clouds and the generated digital terrain model (Wierzbicki *et al*., 2015).

1.3. Orthophotographs

An orthophotograph (orthophoto) is a photogrammetric product that has pictorial qualities of a photograph and the planimetric correctness of a map. They are photographic images constructed from vertical or near-vertical aerial photographs (Amhar *et al*., 1998). The processes used in deriving these orthophotos from aerial images remove the effects of terrain relief displacement and tilt of the aircraft. Because they are planimetrically correct, orthophoto can be used as maps for making direct measurements of distances, angles, positions and areas without making corrections for image displacement (Amhar *et al*., 1998). Orthophotographs are produced by scanning an aerial photo diapositive, ortho-rectifying the digital image and registering it to a coordinate system and map projection (Ngadiman *et al*., 2016). Orthorectification eliminates the effects of tilts and yield an equivalent vertical photograph. The process of removing relief displacements from any perspective photo also removes scale variations and scale becomes constant throughout the photograph. Orthophotos have a number of advantages over conventional maps from their production to their uses. Orthophoto has an interpretative quality inherent in an image and a geometric property of a map. It therefore qualifies as an excellent base or control for GIS. It is relatively less expensive compared with the cost of conventional line mapping. Outputs can either be in hardcopy or stored in a digital form. The orthophoto is an excellent medium for which mapping can be done in inaccessible areas. The digital orthophoto is an excellent vehicle for assessing change in an area (Schickler and Thorpe, 1998).

1.4. Accuracy Assessment of Orthophotographs

Assessment of accuracy of orthophotos can be qualitative or quantitative. Qualitative assessment of orthophotos involve visually inspecting them. Daramola *et al*., (2017) qualitatively assessed the accuracy of orthophoto by overlaying measured features on the digitised features. Visual assessment of the overlaid feature was done by comparing the digitised feature on orthomosaic with the area computed through conventional survey. With a qualitative assessment, minor deformations can be detected on the orthophoto and can further be analysed with the purpose of illustrating the type of error present. Quantitative assessment on the other hand deals with analysing measurement made on the orthophoto. They consist of parameters such as positional and geometric accuracy (Hung *et al*., 2019; Jaud *et al.,* 2016; Harwin and Lucieer, 2012). Positional accuracy includes horizontal and vertical accuracies of checkpoints. Geometric accuracy is also similar to positional accuracy in terms of measurement. The only difference here is that, accuracies are assessed on an object level in geometric accuracy. A number of permanent objects are digitised and measured on an orthophoto and their values are compared with the actual measurements made on the ground (Koeva *et al*., 2018). The accuracy of an orthophoto or any final photogrammetric product is dependent on a number of factors (Hung *et al*., 2019; Gindraux *et al*., 2017). Variation in these factors in either way affects the final accuracy of the product (Gindraux *et al*., 2017; Ruiz *et al*., 2013). These factors range from the data acquisition stage to the production of the final output. Some of the factors which accuracy of orthophotos depend on include: initial image quality; accuracy of GCPs; distribution of GCPs; image overlap (forward and side); flight altitude; camera resolution; and software for processing (Jaud *et al.,* 2016).

2. Materials and Methods

2.1. The Study Area

This study was conducted in the University of Mines and Technology (UMaT) Campus, Tarkwa in the Western Region of Ghana (Figure 1) from August 01 to August 10, 2019. The study area covers about 8 hectares of the campus. The area of study in the University includes the academic area consisting of the various departments and faculties as well as the administrative area of the University (Anon., 2019c). The University of Mines and Technology can be found in a suburb of a mining town in Tarkwa, the managerial capital of the Tarkwa Nsuaem Municipal Assembly in the Western Region of Ghana (Anon., 2019c). The University is geographically located on latitude 5°18′ 00″ N and longitude 1° 59′ 00″ W with an elevation of about 78 m above mean sea level. The University is located about 85 km from Takoradi, the Western Regional capital, 233 km from Kumasi, and about 317 km from Accra (Kesse, 1985). The temperature around the area changes day-to-day with a mean annual temperature of almost 25 °C. Relative humidity ranges from 61% to a maximum of 80% in August and September (Kesse, 1985).

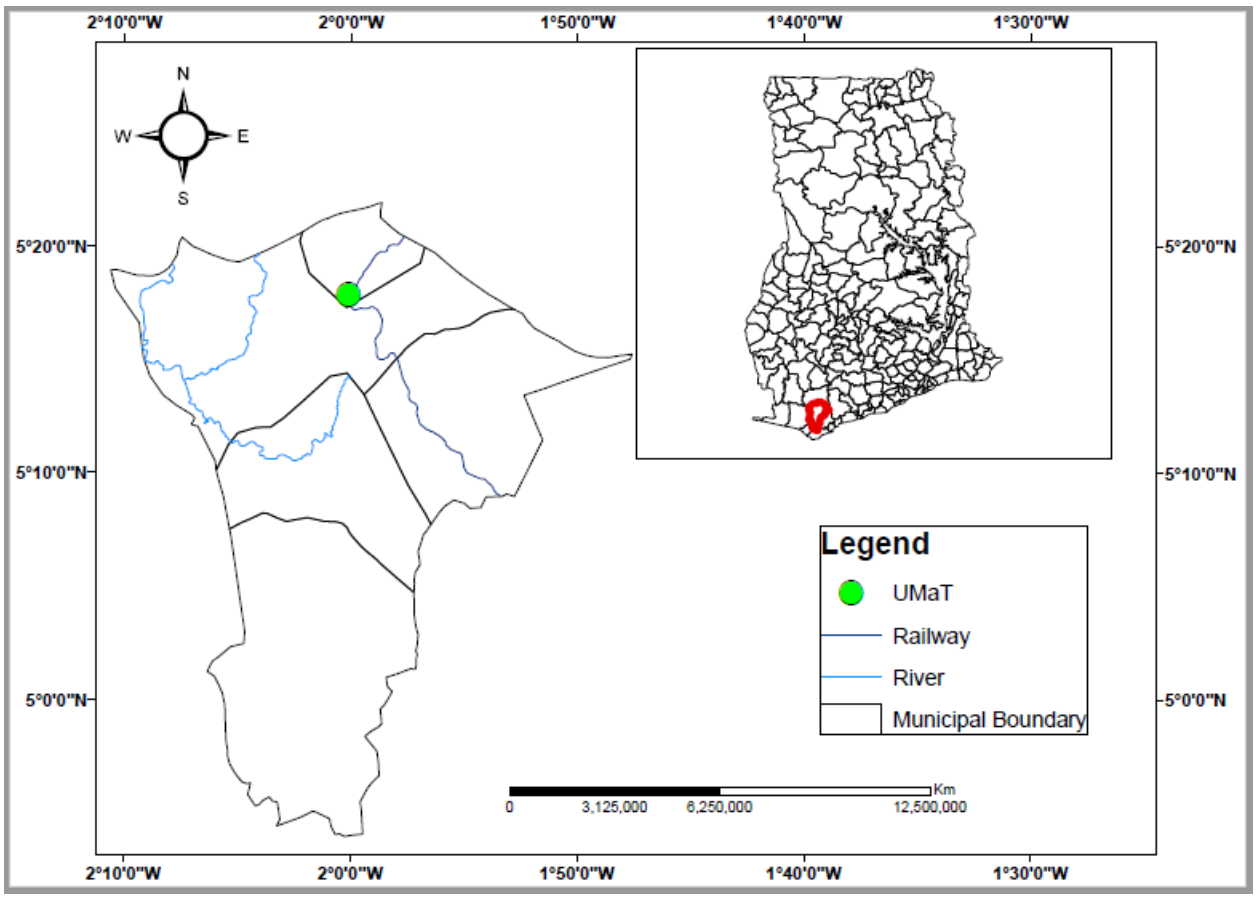

Figure 1 Location of University of Mines and Technology (UMaT) in Tarkwa

2.2. Materials

The materials used in achieving the objectives of this study included GCPs, aerial images, software, Galaxy G1 GNSS equipment and personal computer. The data sources used in this study were entirely primary data. The data included UAV derived images of the area under study as well as

measured ground coordinates of points in the study area. A total number of 127 images per flight were captured with ten (10) GCPs. The software used in this study were Drone deploy and Agisoft Photoscan professional. The primary data was acquired using the following equipment: DJI Phantom 4 Pro Drone with Transmitter (Figure 2); Galaxy G1 GNSS receivers (Figure 3); Clock; Field book and Personal computer.

Figure 2: DJI Phantom 4 Drone with Transmitter

Figure 3 South Galaxy G1 GNSS Receivers

2.3. Methods Used

The methods employed in this study were in four phases. The first phase was the data acquisition process, the second phase was the data processing and orthophoto generation, the third phase was the extraction of coordinates from the orthophotos and the last phase was the accuracy assessment (Figure 4).

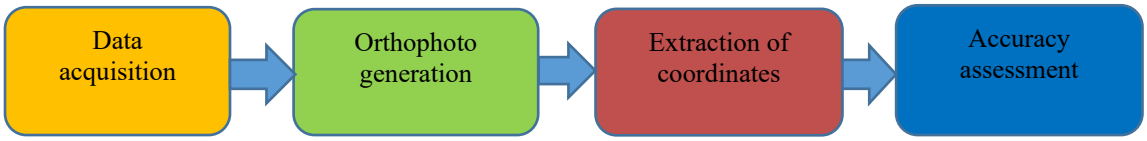

Figure 4 Flow chart of the methods used

2.3.1. Data Acquisition

The data used for this study included surveyed GCPs and aerial images acquired with a UAV (DJI Phantom 4 Pro). Images were acquired three times in a day, for ten (10) days from August 01 to August 10, 2019. Ground coordinates of control points and check points were also determined using static GNSS survey.

Reconnaissance

A preliminary inspection of the study area was first performed. Part of the reconnaissance included identifying an open space that could be used as a safe take-off and landing area. Controls within the study area were also identified to be used as GCPs. Tall buildings, telecommunication masks, electric and network poles, trees and other obstructions were identified and avoided in planning the flight.

Flight Planning

The Drone deploy software was used in planning the mission of the UAV. Parameters set in the drone deploy software remained the same for all flights. Reconnaissance before the mission planning helped in choosing parameters for the flight. Batteries of the drone were fully charged and calibrated before flight. Pre-flight tests were also carried out to ensure proper functioning before proceeding to take-off. Flight lines were designed for the area under study on a digital map embedded in the software. Table 1 shows the parameters used for the flight and image acquisition.

Table 1 Parameters used in planning the flights.

Parameters	Values
Flight height or altitude	80 m
Time of flight	8 min 27 sec
Area covered	8 hectares
Resolution	2.4 cm/px
Front overlap	80%
Side overlap	60%
Flight direction	-123°
Flight speed	6 m/s
Camera angle	90°
Number of images per flight	127

Measurement of Ground Control Points and Check Points

GCPs are included in aerial surveys to enhance the accuracy of the final product and can be avoided or minimised if the UAV has a dual frequency GNSS onboard. Precise survey pillars were used as GCPs. This was due to the fact that GCPs placed on the ground before flight would not persist for the whole period of the image acquisition due to human activities. Conspicuous existing natural and artificial features on the ground were also used as check points (ChPs) considering their clarity on the aerial photographs. The precise coordinates of the control points and check points were all surveyed using differential GNSS technique in the static mode. The coordinates of the GCPs are shown in Table 2. Figures 4, 5 and 6 show the distribution of GCPs and check points in the study area.

Table 2 Coordinates (in UTM Zone 30N) of GCPs and Check Points (ChPs)

Point	Eastings (m)	Northings (m)
GCP 1	610584.68	585780.05
GCP 2	610762.62	585901.24
GCP 3	610800.03	585646.13
GCP 4	610738.67	585740.22
GCP 5	610822.68	585809.09
GCP 6	610762.49	585776.80
ChP 1	610683.32	585818.73
ChP 2	610705.25	585701.48
ChP 3	610723.83	585653.86
ChP 4	610839.18	585707.13

Image Acquisition

The image acquisition started from 8:00 am to 5:30 pm spanning a period of ten (10) days from August 01 to August 10, 2019. In preparation for the flight, the UAV, the Radio Connection (RC) transmitter and an iPad tablet were connected. The drone only took-off after ensuring that all checklists have been verified. These checklists consisted of: Connection of transmitter (controller) to drone; Drone GPS satellites; Camera is ready; Drone is calibrated; and Mission uploaded to drone. Other important factors such as the battery levels for both the transmitter and drone among others were also checked. The drone images of the study area were acquired three times a day (i.e. Morning: between 8 and 8:15 am; Afternoon: between 1:30 to 2:00 pm and Evening: between 5:00 to 5:30 pm) for ten days. During the aerial survey, the number of satellites visible to the onboard GNSS ranged between 15 to 19.

2.3.2. Orthophoto Generation (Data Processing)

Data processing and orthophoto generation was done using an Agisoft PhotoScan professional Software. Series of procedures were undertaken in the software before the orthophotos were produced. The first step in creating the orthophotos was to load the UAV acquired images in the Agisoft PhotoScan. It involved selecting images from the appropriate folder for further processing. For this study, thirty different sets of UAV images were loaded into the PhotoScan for processing separately. However, parameters set before the loading of images at the PhotoScan preferences remained the same throughout the processing. The next step after adding photos in the software was to align the uploaded images. At this stage PhotoScan finds the camera position and orientation for each photo and builds a sparse point cloud model. In Agisoft, alignment is done with the Structure for Motion (SfM), technique. SfM detects geometrical similarities with specific details that serve as image feature points. The movement of these points throughout the whole sequence in the workspace is thereby monitored giving an estimation of feature point positions and subsequently rendered as three-dimensional point cloud. When these are identified, PhotoScan refines camera calibration parameters to create point cloud data and a set of camera positions (Verhoeven, 2011). PhotoScan allows to generate and visualise a Digital Elevation Model (DEM). A DEM was rasterised from the dense point cloud for higher accuracy. DEM is required in the production of orthophoto since PhotoScan uses the Triangular Irregular Network (TIN) surface to correct for displacement and calculated exterior orientations for georeferencing in the orthorectification process (Anon., 2012 Ruiz *et al*., 2013). Orthomosaic were built based on the generated DEM.

2.3.3. Extraction of Coordinates and Accuracy Assessment

Horizontal coordinates of ground features were extracted from the orthophotos and compared with coordinates of the same features measured using static GNSS receivers on the ground to determine the positional accuracy of the orthophotos. The positional accuracies of the ground features were determined by calculating Root Mean Square Error (RMSE) of the coordinate differences between

features on orthophotos and the GNSS measured points in X, Y as well as the total RMSE, using Equations 1, 2 and 3 respectively.

$$RMSE_x = \sqrt{(\Sigma(\Delta \mathbf{X})^2}/n) \quad [1]$$

$$RMSE_y = \sqrt{(\Sigma(\Delta \mathbf{Y})^2}/n) \quad [2]$$

$$\text{Total RMSE} = \sqrt{(RMSE_x)^2 + (RMSE_Y)^2} \quad [3]$$

3. Results and Discussions

3.1. Results

Thirty orthophotos in all were produced from the thirty sets of images acquired in the study area. Orthophotos of day One (1) are shown in Figures 5 to 7. Orthophotos were thus produced for the study area from morning, afternoon and evening UAV images, for ten (10) days. After processing the images, analysis was performed on all the orthophotos. The analysis considered the positional accuracies of the orthophotos as well as the spatial resolution of the maps obtained. Table 6 presents results of the RMSE calculations for all the ten (10) days of observations.

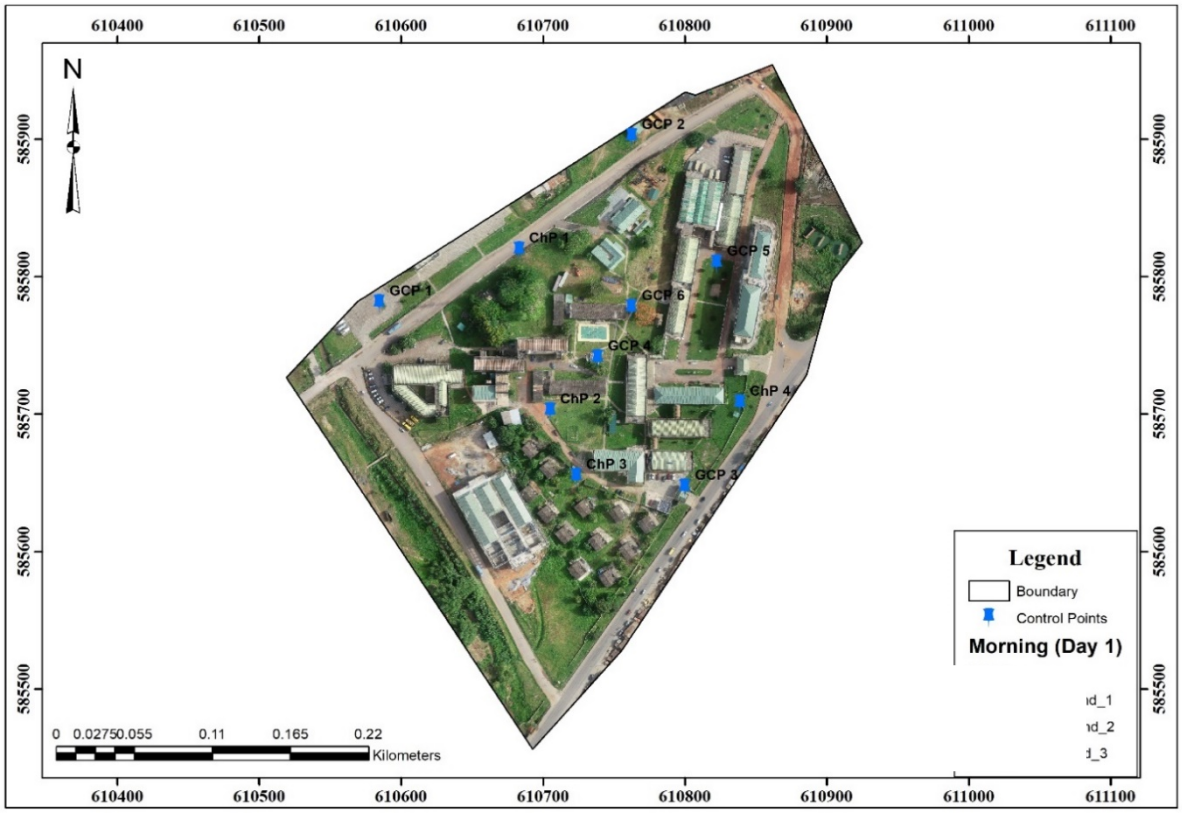

Figure 5: Day 1 Morning Orthophoto with Distribution of GCPs

Table 3: Coordinates and Statistics of Day 1 Morning Orthophoto

	GNSS		Orthophoto		Difference		Squared Errors	
ID	**X**	**Y**	**X**	**Y**	**ΔX**	**ΔY**	**ΔX^2**	**ΔY^2**
GCP 1	610584.68	585780.05	610584.61	585780.02	0.07	0.03	0.0049	0.0009
GCP 2	610762.62	585901.24	610762.61	585901.25	0.01	-0.01	0.0001	0.0001
GCP 3	610800.03	585646.13	610800.09	585646.15	-0.06	-0.02	0.0036	0.0004
GCP 4	610738.67	585740.22	610738.62	585740.40	0.05	-0.18	0.0025	0.0324
GCP 5	610822.68	585809.09	610822.64	585809.19	0.04	-0.10	0.0016	0.0100
GCP 6	610762.49	585776.80	610762.40	585776.60	0.09	0.20	0.0081	0.0400
ChP 1	610683.32	585818.73	610683.21	585818.55	0.11	0.18	0.0121	0.0324
ChP 2	610705.25	585701.48	610705.42	585701.32	-0.17	0.16	0.0289	0.0256
ChP 3	610723.83	585653.86	610723.92	585653.78	-0.09	0.08	0.0081	0.0064
ChP 4	610839.18	585707.13	610839.21	585707.12	-0.03	0.01	0.0009	0.0001
					Total Error		**0.0708**	**0.1483**
					RMSEx; RMSEy		**0.0841**	**0.1218**
					Total RMSE		**0.01643**	

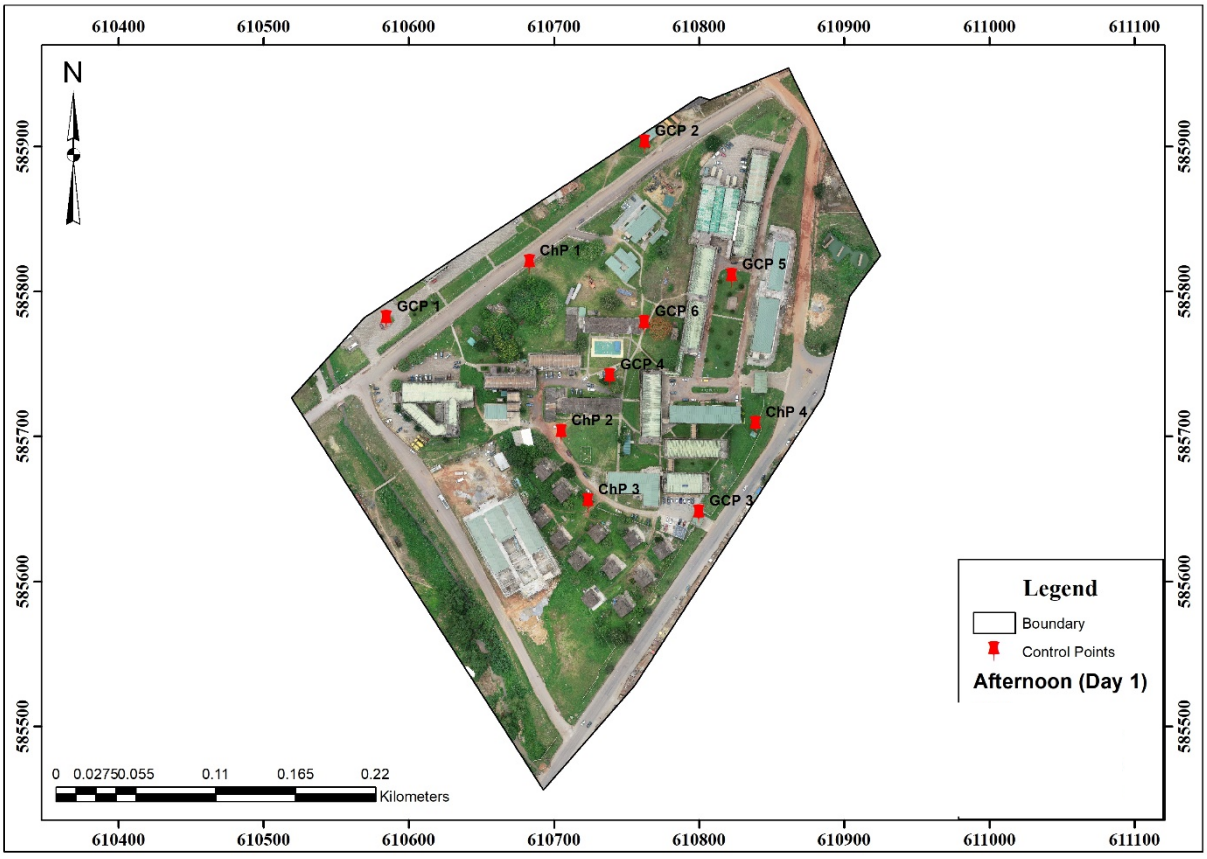

Figure 6: Day 1 Afternoon Orthophoto with Distribution of GCPs

Table 4: Coordinates and Statistics of Day 1 Afternoon Orthophoto

	GNSS		Orthophoto		Difference		Squared Errors	
ID	**X**	**Y**	**X**	**Y**	**ΔX**	**ΔY**	**ΔX^2**	**ΔY^2**
GCP 1	610584.68	585780.05	610584.21	585780.10	0.47	-0.05	0.2209	0.0025
GCP 2	610762.62	585901.24	610762.43	585901.12	0.19	0.12	0.0361	0.0144
GCP 3	610800.03	585646.13	610800.32	585646.11	-0.29	0.02	0.0841	0.0004
GCP 4	610738.67	585740.22	610738.64	585740.10	0.03	0.12	0.0009	0.0144
GCP 5	610822.68	585809.09	610822.45	585809.13	0.23	-0.04	0.0529	0.0016
GCP 6	610762.49	585776.80	610762.30	585776.34	0.19	0.46	0.0361	0.2116
ChP 1	610683.32	585818.73	610683.25	585818.60	0.07	0.13	0.0049	0.0169
ChP 2	610705.25	585701.48	610705.41	585700.40	-0.16	1.08	0.0256	1.1664
ChP 3	610723.83	585653.86	610724.32	585654.16	-0.49	-0.30	0.2401	0.0900
ChP 4	610839.18	585707.13	610839.40	585707.01	-0.22	0.12	0.0484	0.0144
					Total Error		**0.7500**	**1.5326**
					RMSEx; RMSEy		**0.6878**	**1.0263**
					Total RMSE		**1.1546**	

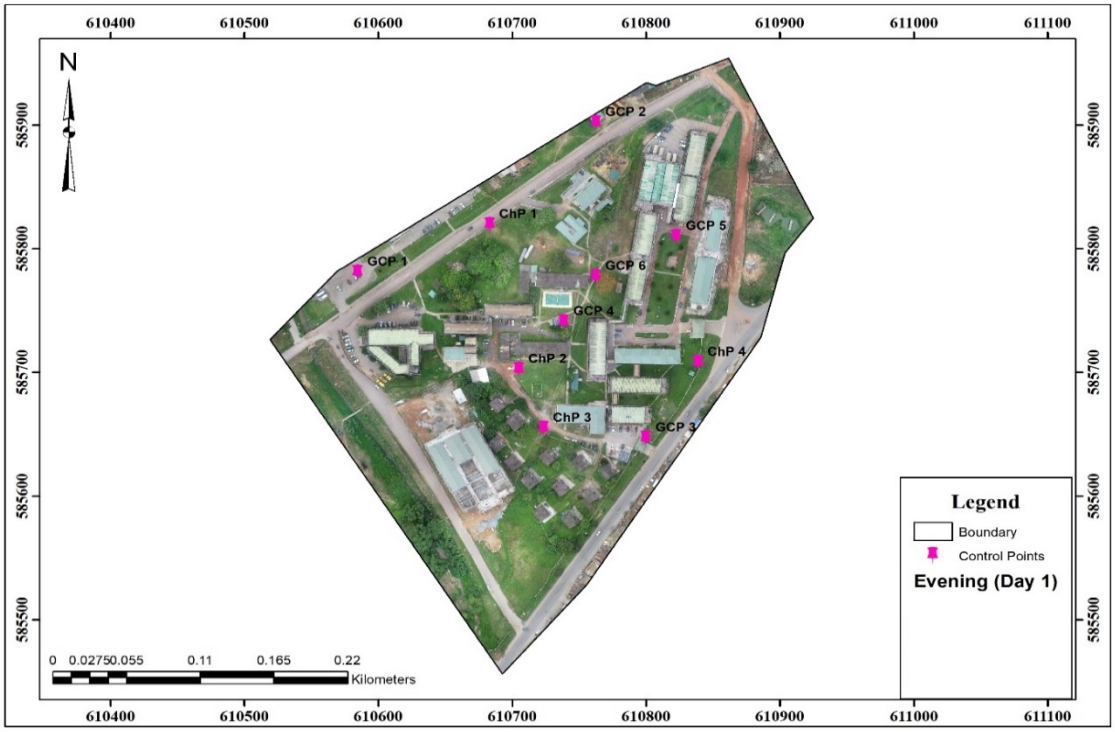

Figure 7: Day 1 Evening Orthophoto with Distribution of GCPs

Table 5: Coordinates and Statistics of Day 1 Evening Orthophoto

	GNSS		Orthophoto		Difference		Squared Errors	
ID	**X**	**Y**	**X**	**Y**	**ΔX**	**ΔY**	**ΔX^2**	**ΔY^2**
GCP 1	610584.68	585780.05	610584.28	585780.08	0.40	-0.03	0.1600	0.0009
GCP 2	610762.62	585901.24	610762.69	585901.20	-0.07	0.04	0.0049	0.0016
GCP 3	610800.03	585646.13	610800.54	585646.15	-0.51	-0.02	0.2601	0.0004
GCP 4	610738.67	585740.22	610738.23	585740.43	0.44	-0.21	0.1936	0.0441
GCP 5	610822.68	585809.09	610822.55	585809.16	0.13	-0.07	0.0169	0.0049
GCP 6	610762.49	585776.80	610762.46	585776.29	0.03	0.51	0.0009	0.2601
ChP 1	610683.32	585818.73	610684.28	585818.56	-0.96	0.17	0.9216	0.0289
ChP 2	610705.25	585701.48	610705.49	585701.23	-0.24	0.25	0.0576	0.0625
ChP 3	610723.83	585653.86	610724.43	585654.21	-0.60	-0.35	0.3600	0.1225
ChP 4	610839.18	585707.13	610839.41	585707.25	-0.23	-0.12	0.0529	0.0144
					Total Error		**2.0285**	**0.5403**
					RMSEx; RMSEy		**0.7147**	**1.2248**
					Total RMSE		**1.5846**	

Table 6: RMSE Values for Morning, Afternoon and Evening Orthophotos

Day	RMSE	Morning observation	Afternoon observation	Evening observation
1	RMSEx	**0.0841**	**0.6878**	**0.7147**
	RMSEy	**0.1218**	**1.0263**	**1.2248**
	Total RMSE	**0.01643**	**1.1546**	**1.5846**
2	RMSEx	**0.0835**	**0.6543**	**0.6763**
	RMSEy	**0.0812**	**1.3054**	**1.1267**
	Total RMSE	**0.0096**	**1.7571**	**1.3493**
3	RMSEx	0.**0614**	**0.7837**	**0.6736**
	RMSEy	**0.0530**	**1.2494**	**1.1590**
	Total RMSE	**0.0047**	**1.6773**	**1.4179**
4	RMSEx	**0.0983**	**0.8228**	**0.6819**
	RMSEy	**0.1474**	**1.3309**	**1.2703**
	Total RMSE	**0.0283**	**1.8961**	**1.6794**
5	RMSEx	**0.0864**	**0.6560**	**0.6697**
	RMSEy	**0.1104**	**1.1519**	**1.2676**
	Total RMSE	**0.0143**	**1.4108**	**1.6681**
6	RMSEx	**0.1471**	**0.6429**	**0.6734**
	RMSEy	**0.0976**	**1.2499**	**1.2077**
	Total RMSE	**0.0236**	**1.6161**	**1.5274**
7	RMSEx	**0.0923**	**0.6691**	**0.6717**
	RMSEy	**0.1032**	**1.1291**	**1.1050**
	Total RMSE	**0.0136**	**1.3518**	**1.3019**
8	RMSEx	**0.1507**	**0.6603**	**0.6725**
	RMSEy	**0.1256**	**1.2606**	**1.1405**
	Total RMSE	**0.0276**	**1.6478**	**1.3771**
9	RMSEx	**0.1339**	**0.6619**	**0.6553**
	RMSEy	**0.1254**	**1.1555**	**1.2579**
	Total RMSE	**0.0238**	**1.4052**	**1.6396**
10	RMSEx	**0.1005**	**0.4070**	**0.4330**
	RMSEy	**0.1432**	**0.6162**	**0.4274**
	Total RMSE	**0.0229**	**0.4142**	**0.2618**

3.2. Discussions

From the results, the Total RMSE for morning ranged from 0.0047 m to 0.0283 m, the Afternoon total RMSEs ranged from 0.4152 m to 1.8961 m and Evening total RMSEs ranged from 0.2618 m to 1.6794 m. According to the American Society of Photogrammetry and Remote Sensing (ASPRS, 2015) (Anon., 2015), the recommended horizontal accuracy class for RMSEx and RMSEy for high accuracy work should be within 0.025 m and a Total RMSE should not be more than 0.035 m for a spatial resolution of 2.5 cm. Also, for standard mapping and GIS work, the recommended horizontal accuracy class for RMSEx and RMSEy should be within 0.05 m and a Total RMSE should not be more than 0.071 m for a spatial resolution of 2.5 cm. The coordinates derived from UAV images taken in the morning with average temperatures between 21 ℃ and 23 ℃ with average wind speed of not more than 10 m/s gave the lowest RMSE (highest accuracy) followed by images taken in the evening and afternoon respectively. Therefore, orthophotos derived from morning UAV images averagely gave the highest positional accuracy (Table 6).

4. Conclusions

From the results, it can be concluded that, the positional accuracies (using horizontal coordinates) of orthophotos derived from UAV images captured during early hours of the day (i.e. morning) with average temperatures between 21 ℃ and 23 ℃ with average wind speed of not more than 10 m/s are suitable for high accuracy work. Consequently, airborne high-resolution UAVs are a promising technology that can be used to acquire high quality aerial photos at a relatively short time and at a cheaper cost compared to conventional aerial photogrammetry. However, metric cameras should be used to maintain high degree of accuracies. It is therefore recommended that for high accuracy work, UAV surveys should be done during the early hours of the day (Morning) with average temperatures between 21 ℃ and 23 ℃ with average wind speed of not more than 10 m/s for UAV weights within 1.5 kg. Also, GCPs should be used during the generation of orthophotos and not after their production.

5. References

Abubakar, T., Babayo, A. and Umar, S. (2017), "Time Optimization for GPS Observation using GNSS Planning.", *International Journal of Innovative Research in Technology*, *Basic and Applied Sciences ISSN Print: 2465-7301 | ISSN Online*, pp. 2467-8171.

Amhar, F., Josef, J., C. Ries (1998). The Generation of True Orthophotos Using a 3D Building Model in Conjunction with a Conventional DTM, *International Archives of Photogrammetry and Remote Sensing*, vol.32, Part 4, pp. 16-22.

Anon. (2012), "Agisoft PhotoScan – Capabilities", *www.agisoft.ru/w/index.php?title=PhotoScan/Capabilities*, Accessed: March 2, 2019.

Anon. (2014), "How Does Weather Affect Surveying", www.schneidercorp.com. Accessed: January 27, 2019.

Anon. (2015), "New Standard for New Era: Overview of the 2015 ASPRS Positional Accuracy Standards for Digital Geospatial Data", *Photogrammetric Engineering and Remote Sensing* Vol. 81, No. 3, pp. 173-176.

Anon. (2019a), "Accuracy of Surveying", *www.landsurveyors.com*. Accessed: January 27, 2019.

Anon. (2019b), "Weather, Season and the Land Surveyor", *www.tnlds.com*. Accessed: January 27, 2019.

Anon. (2019c), "University of Mines and Technology", *www.google.com*. Accessed: February 8, 2019.

Blyenburgh, P. (1999), "UAVs and Overview", *Air & Space Europe*, Vol. I, pp. 43-47.

Chauhan, D. S., Srivastava, S. K., Chandra, A. M. (2006), "Plane Surveying", *New Age International Pvt Ltd Publishers, SBN-13: 978-81-224-1902-3, ISBN: 81-224-1902-X,* 602pp.

Colomina, I. and Molina, P. (2014), "Unmanned Aerial Systems for Photogrammetry and Remote Sensing: A Review", *ISPRS Journal of Photogrammetry and Remote Sensing*, Vol. 92, pp. 79-97.

Daramola, O., Olaleye, J., Ajayi, O.G. and Olawuni, O. (2017), "Assessing the Geometric Accuracy of UAV-Based Orthophotos", *South African Journal of Geomatics*, Vol. 6, No. 3, pp. 395-406.

Eisenbeiss, H. (2009), "UAV photogrammetry", Ph.D. Thesis, Institut für Geodesie und Photogrammetrie, Zürich, Switzerland, 237pp.

Everaerts, J. (2008), "The Use of Unmanned Aerial Vehicles (UAVS) for Remote Sensing and Mapping", *The International Archives of the Photogrammetry, Remote Sensing and Spatial Information Sciences, ISPRS* Congress, Beijing, China, pp.1187-1192.

Gindraux S., Boesch R. and Farinotti D. (2017), "Accuracy Assessment of Digital Surface Models from Unmanned Aerial Vehicles' Imagery on Glaciers", *Remote Sensing*, No. 9, 186pp.

Hakala, T., Honkavaara, E., Saari, H., Mäkynen, J., Kaivosoja, J., Pesonen, L. and Pölönen, I. (2013), "Spectral Imaging from UAVs Under Varying Illumination Conditions", *International Archives of the*

Photogrammetry, Remote Sensing and Spatial Information Sciences, ISPRS, Vol. XL-1/W2, UAV-g2013, pp. 189-194.

Harwin, S. and Lucieer, A. (2012), "Assessing the Accuracy of Georeferenced Point Clouds Produced Via Multi-View Stereopsis from Unmanned Aerial Vehicle (UAV) Imagery", *Remote Sensing*, Vol. 4, No. 6, pp. 1573–1599.

Hung I.-K., Unger D., Kulhavy D. and Zhang Y. (2019), "Positional Precision Analysis of Orthomosaics Derived from Drone Captured Aerial Imagery", *Drones*, No. 3, 46pp.

Jaud M., Passot S., Le Bivic R., Delacourt C., Grandjean P., Le and Dantec N. (2016), "Assessing the Accuracy of High Resolution Digital Surface Models Computed by PhotoScan® and MicMac® in Sub-Optimal Survey Conditions", *Remote Sensing*, No. 8, 465pp.

Kesse, G. O. (1985), The Mineral and Rock Resources of Ghana, A. A. Balkema, Rotterdam, 610 pp.

Koeva, M., Muneza, M., Gevaert, C., Gerke, M. and Nex, F. (2018), "Using UAVs for Map Creation and Updating: A Case Study in Rwanda", *Survey Review*, Vol. 50, No. 361, pp. 312-325.

Leitão, J.P., Moy de Vitry, M., Scheidegger, A. and Rieckermann, J. (2016), "Assessing the Quality of Digital Elevation Models Obtained from Mini Unmanned Aerial Vehicles for Overland Flow Modelling in Urban Areas" *Hydrology and Earth System Sciences*, Vol. 20, No. 4, pp.1637-1653.

Mantey, S. and Tagoe, N. D., (2019), "Suitability of Unmanned Aerial Vehicles for Cadastral Surveys", *Ghana Mining Journal,* Vol. 19, No. 1, pp. 1 - 8.

Manyoky, M. Theiler, P. Steudler, D. and Eisenbeiss, H. (2011), Unmanned Aerial Vehicle in Cadastral Applications, International Archives of the Photogrammetry, Remote Sensing and Spatial Information Sciences, Volume XXXVIII-1/C22, 2011ISPRS Zurich 2011 Workshop, 14-16 September 2011, Zurich, Switzerland,57pp.

Ngadiman, N., Kaamin, M., Sahat, S., Mokhtar, M., Ahmad, N.F.A., Kadir, A.A. and Razali, S.N.M. (2016), "Production of Orthophoto Map Using UAV Photogrammetry: A Case Study in UTHM Pagoh Campus", *American Institute of Physics Conference Proceedings*, Vol. 2016, No. 1, pp. 1-6.

Raczynski, R.J., (2017), "Accuracy analysis of products obtained from UAV-borne photogrammetry influenced by various flight parameters", Master's thesis, NTNU, 80pp.

Ruiz, J. J., Diaz-Mas, L., Perez, F. and Viguria, A. (2013), "Evaluating the Accuracy of DEM Generation Algorithms from UAV imagery", *The International Archives of the Photogrammetry, Remote Sensing and Spatial Information Sciences*, Rostock, Germany, Vol. XL-1/W2, UAV-g2013, pp. 333-337.

Schickler, W. and Thorpe, A., (1998), "Operational Procedure for Automatic True Orthophoto Generation", *International Archives of Photogrammetry and Remote Sensing*, Vol. 32, Part 4, pp. 527-532.

Thomas, H. (2016), "Quantitative Analysis of Two Low-Cost Aerial Photography Platforms: A Case Study of "the Site of Zagora, Andros, Greece", *Journal of Field Archaeology*, Vol. 9, No. 4, pp. 38-46.

Verhoeven, G. (2011), "Taking computer vision aloft – archaeological three-dimensional reconstructions from aerial photographs with PhotoScan", *Archaeological Prospection*, Vol. 18 No.1, pp. 67–73.

Volkmann W. and Barnes G., (2014), "Virtual Surveying: Mapping and Modeling Cadastral Boundaries Using Unmanned Aerial Systems (UAS)," (paper presented at the XXV FIG Congress, Kuala Lumpur, Malaysia, June 16-21, 13pp.

Wierzbicki, D., Kedzierski, M. and Fryskowska, A. (2015), "Assessment of the Influence of UAV Image Quality on the Orthophoto Production" *The International Archives of Photogrammetry, Remote Sensing and Spatial Information Sciences*, Vol. 40, No. 1, 8pp.